INITIAL RESULTS IN PRONY ANALYSIS OF POWER SYSTEM RESPONSE SIGNALS

J.F. Hauer
Senior Member

C.J. Demeure
Member

L.L. Scharf
Fellow

BONNEVILLE POWER ADMINISTRATION
PORTLAND, OREGON

THE UNIVERSITY OF COLORADO
BOULDER, COLORADO

Abstract

Prony analysis is an emerging methodology that extends Fourier analysis by directly estimating the frequency, damping, strength, and relative phase of modal components present in a given signal. The ability to extract such information from transient stability program simulations and from large-scale system tests or disturbances would be quite valuable to power system engineers. This paper reports early results in the application of this method to stability program output. It also includes benchmarks against known models and a brief mathematical summary.

Keywords: Prony, signal analysis, modal analysis, dynamics, stability, eigenvalue, singular value

I. INTRODUCTION

Prony analysis [1-11] is an emerging methodology that extends Fourier analysis by directly estimating the frequency, damping, strength, and relative phase of modal components present in a given signal. The ability to extract such information from transient stability program (TSP) simulations and from large-scale system tests or disturbances would be very useful to power system engineers.

Such a tool would be particularly valuable for TSP output analysis, where it could provide

- o parametric summaries for damping studies (data compression)
- o quantified information for adjusting remedial controls (sensitivity analysis and performance evaluation)
- o insight into modal interaction mechanisms (modal analysis)
- o reduced simulation times for damping evaluation (prediction)

These considerations lead BPA to contract with Dr. Louis Scharf for the writing of a FORTRAN program based upon his research into Prony methods. The effort was lead by Dr. Cedric Demeure, who produced the interactive FORTRAN program DTRANSCIENT.

89 SM 702-2 PWRS A paper recommended and approved by the IEEE Power System Engineering Committee of the IEEE Power Engineering Society for presentation at the IEEE/PES 1989 Summer Meeting, Long Beach, California, July 9 - 14, 1989. Manuscript submitted January 26, 1989; made available for printing May 23, 1989.

BPA has since made substantial changes to DTRANSCIENT. The objectives are to evaluate the method, to revise the code for utility applications, and to fortify both for use with large models. Polynomial rooting, a critical and numerically demanding task, is now accomplished by a routine that was extracted from the NASA program SAMSAN [12] and converted to quadruple precision. The revised DTRANSCIENT has been combined with comprehensive driving logic to form SIGPAKZ. This program closely parallels the BPA Fourier analysis programs SIGPAK [13] and SIGPAKR [14]. All three readily accept signal data from the BPA TSP, BPA's Power System Disturbance Monitor amd variety of special sources.

This paper reports early results in the application of SIGPAKZ to power system problems. It also includes benchmarks against known models and a brief mathematical description of Prony analysis.

II. A BRIEF DESCRIPTION OF PRONY'S METHOD

Like Fourier analysis, what we shall call Prony analysis originated in an earlier century [1]. Its practical use has awaited the digital computer, and means for dealing with some inherently ill-conditioned mathematics.

Suppose that a linear, time-invariant dynamic system is brought to an "initial" state $x(t_o)=x_o$ at time t_o, by means of some test input or disturbance. Then, if the input is removed and there are no subsequent inputs or disturbances to the system, it will "ring down" according to a differential equation of form

$$\dot{x} = A\,x \tag{1}$$

where x is the state of the system and n is the number of components in x (i.e., the order of the system). Let λ_i, p_i, q_i^T be respectively the eigenvalues, right eigenvectors, and left eigenvectors of (n x n) matrix A. (See [15] or [16] for details). Then the solution to (1) can be expressed as

$$x(t) = \sum_{i=1}^{n} (q_i^T x_o)\, p_i \exp(\lambda_i t) \tag{2A}$$

$$= \sum_{i=1}^{n} R_i x_o \exp(\lambda_i t) \tag{2B}$$

where $R_i = p_i q_i^T$ is an (n x n) residue matrix. Note that $q_i^T x_o$ in (2A) is scalar (that is, a simple constant). This implies that, though x_o (with q_i^T) determines the stimulus to the mode associated with eigenvalue λ_i, the distribution of modal response among the components of x is entirely determined by the corresponding right eigenvector p_i. Consequently information about p_i can be extracted by an appropriate modal decomposition of x(t).

For simplicity, suppose that there is just one output from the system and that it is of form

$$y(t) = C\,x(t). \tag{3}$$

Prony methods and their recent extensions are designed to directly estimate the parameters for the exponential terms in (2A) and/or (3), by fitting a function

$$\hat{y}(t) = \sum_{i=1}^{Q} A_i \exp(\sigma_i t)\cos(2\pi f_i t + \phi_i) \tag{4}$$

to an observed record for y(t). In doing this it may also be necessary to model offsets, trends, noise, and other extraneous effects in the signal.

Let the record for y(t) consist of N samples $y(t_k)=y(k)$, $k=0,1,\ldots,N-1$, that are evenly spaced by an amount Δt. The strategy for obtaining a Prony solution (PRS) can be summarized as follows:

STEP 1: construct a discrete linear prediction model (LPM) that fits the record.

STEP 2: find the roots of the characteristic polynomial associated with the LPM of step 1.

STEP 3: using the roots of step 2 as the complex modal frequencies for the signal, determine the amplitude and initial phase for each mode.

These steps are performed in z-domain. For power system applications the eigenvalues would usually be translated to s-domain, consistent with equations (1)-(5).

Prony's main contribution is at step 1. Its development here parallels that of [2], pp. 378 and 379. For initial purposes, assume N=2n and that the signal record is noise-free.

The notation is simplified if (4) is recast in the exponential form

$$\hat{y}(t) = \sum_{i=1}^{P} B_i \exp(\lambda_i t) \tag{5}$$

paralleling (2). At the sample times t_k this can be contracted to

$$\hat{y}(k) = \sum_{i=1}^{P} B_i z_i^k, \tag{6A}$$

$$z_i = \exp(\lambda_i \Delta t). \tag{6B}$$

The immediate objective is to find the B_i and z_i that produces $\hat{y}(k)=y(k)$ for all k. For insight as to how this can be done, apply (6A) at each t_k and form the following equation:

$$\begin{bmatrix} B_1 z_1^0 + \ldots + B_n z_n^0 \\ B_1 z_1^1 + \ldots + B_n z_n^1 \\ \vdots \\ B_1 z_1^{N-1} + \ldots + B_n z_n^{N-1} \end{bmatrix} = \begin{bmatrix} z_1^0 & z_2^0 & \ldots & z_n^0 \\ z_1^1 & z_2^1 & \ldots & z_n^1 \\ \vdots & \vdots & & \vdots \\ z_1^{N-1} & z_2^{N-1} & \ldots & z_n^{N-1} \end{bmatrix} \begin{bmatrix} B_1 \\ B_2 \\ \vdots \\ B_{N-1} \end{bmatrix} = \begin{bmatrix} y(0) \\ y(1) \\ \vdots \\ y(N-1) \end{bmatrix} \tag{7A}$$

This can be expressed more compactly as

$$ZB = Y. \tag{7B}$$

If the z_i are found then the eigenvalues λ_i can be calculated from them via (6B). The z_i are necessarily the roots of some nth-order polynomial with (unknown) coefficients a_i, and thus satisfy

$$z^n - (a_1 z^{n-1} + a_2 z^{n-2} + \ldots + a_n z^0) = 0 \tag{8}$$

Next construct the (1 x N) matrix

$$\bar{A} = [-a_n\ -a_{n-1}\ \ldots\ -a_1\ 1\ 0\ \ldots\ 0] = [-a\ 1\ 0] \tag{9}$$

and apply it to (7): after some minor reordering,

$$\begin{aligned} \bar{A}Y &= y(n) - [a_1 y(n-1) + \ldots + a_n y(0)] \\ &= \bar{A}ZB \\ &= B_1[z_1^n - (a_1 z_1^{n-1} + a_2 z_1^{n-2} + \ldots + a_n z_1^0)] + \ldots \\ &= 0 \end{aligned} \tag{10}$$

where the last step follows from the fact that each z_i satisfies (8). Since the initial time has been selected arbitrarily, (10) can be applied repeatedly to form

$$\begin{bmatrix} y(n-1) & y(n-2) & \ldots & y(0) \\ y(n-0) & y(n-1) & \ldots & y(1) \\ y(n+1) & y(n-0) & \ldots & y(2) \\ \vdots & \vdots & & \vdots \\ y(N-2) & y(N-3) & \ldots & y(N-n-1) \end{bmatrix} \begin{bmatrix} a_1 \\ a_2 \\ \vdots \\ a_n \end{bmatrix} = \begin{bmatrix} y(n+0) \\ y(n+1) \\ y(n+2) \\ \vdots \\ y(N-1) \end{bmatrix} \tag{11}$$

Solution of this equation provides the z-domain polynomial in (8), which is then rooted for the z_i and, through (6B), the eigenvalues λ_i. This completes steps 1 and 2 of the basic Prony method. Step 3 is the solution of (7) for the complex amplitudes B_i.

Practical use of this approach requires some extensions and refinements. A major problem is that the true system dimension, n, may be unknown or may be so large that any fitted model must be a reduced-order approximation. Additional modes may be needed to fit signal offsets or noise. The array dimensions in (11) will usually differ from those shown, and tend to "overfit" the signal by using a generous number of samples and fitted modes. Singular-value analysis and other mechanisms are then used to adjust model features at each solution step.

The reconstructed signal y(t) will usually fit y(t) inexactly. An appropriate measure for the quality of this fit, used here, is the signal-to-noise ratio

$$SNR = 20 \log ||y(k)-\hat{y}(k)||/||y(k)|| \qquad (12)$$

where $||.||$ denotes the usual root-mean-square norm and the SNR is in decibels (dB).

III. STRATEGIC ISSUES

The immediate objective is to assess Prony analysis as a tool for power system applications, and to conduct or promote further development as needed. There are many aspects to this. The methodology itself permits many variations. Then, for a given record, there are questions as to

- o preprocessing, to mitigate the effects of noise or hidden inputs
- o how much of the record to use in the model fit
- o the order of the fitted model
- o pruning and/or adjustment of the fitted model

The power system models ordinarily used in stability studies pose serious difficulties for Prony analysis (and for other methods that rely upon linearization). They are strongly nonlinear, and of dimensions well beyond those of models that any fitting procedure would reliably construct. Linear characterizations can be developed for power system transient behavior, but, if they are formed with respect to the actual operating point, they should be expected to vary with time. It appears that Prony analysis performs such a characterization implicitly.

The evaluation of Prony analysis in this context requires special attention to the factors below:

- o The Prony model will normally be of far lower order than the dynamic process underlying the signal record.
- o For large-signal cases, PRS results will change with the magnitude of the system disturbance or input.
- o For large-signal cases, PRS results will change with record length and position.
- o For large-signal cases, there is probably a maximum record length beyond which information is lost in the PRS.
- o For small-signal cases, substantial changes in record length should not produce material changes in PRS results.

These are being examined through a series of test cases, which range from very simple to rather difficult. Salient results are presented in the sections that follow.

The methodology is also being applied to system operating records, in a parallel effort. In this environment the problems with noise and hidden inputs are much more severe, and alternative methods (such as lattice filters [17-19]) may be also be tested.

IV. PRS CHECK SERIES #0

This series of checks is based upon two elementary models. The first of these, shown in Figure 1, has two complex modes. Both have zero damping. Model #2 has the same structure and parameters, except that the 0.67 Hz mode has a damping of 0.02 and the

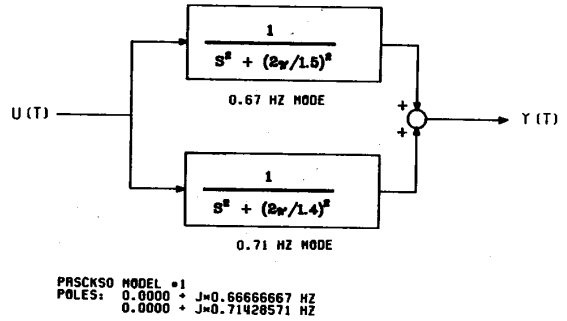

Fig. 1. Model #1 for prs check series #0

0.71 Hz mode has a damping of -0.005. The unit for damping here is inverse seconds, divided by 2π to be dimensionally consistent with frequency in Hz.

Model #1 was introduced in [20], as a proposed benchmark for damping estimators. The modal frequencies are realistic for the western power system, and there is a risk that the modal damping may be so as well. Figure 2 illustrates that the direct examination of such damping can require very long simulations for correct results. A hoped-for benefit of Prony analysis is the minimization of simulation length.

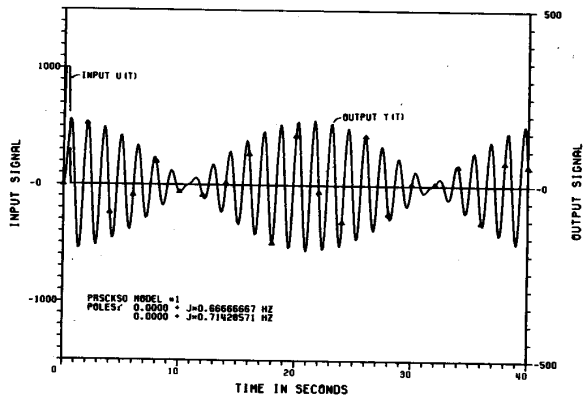

Fig. 2. Response of PRSCKSo model #1 to brief pulse input

Prony analysis was performed on the Figure 2 signal for successively longer values of the record length, TBAR. In all cases the sample spacing was Δt=0.10 sec. The solution logic, though permitted to develop a model of order 90, in each case recognized that just two significant (complex) modes were present and pruned the initial LPM accordingly. Model parameter estimates were accurate to 4 significant digits for a 2 second record, and improved with record length. Like results were obtained for Model 2.

V. PRS CHECK SERIES #4

The basic model for PRS check series #4 has the frequency response shown in Figure 3A. It represents a linear characterization of bus frequency response to small-signal control action during a major disturbance (see [21], Section V). Having 14 complex modes, it is of order n=28. Some modes are closely

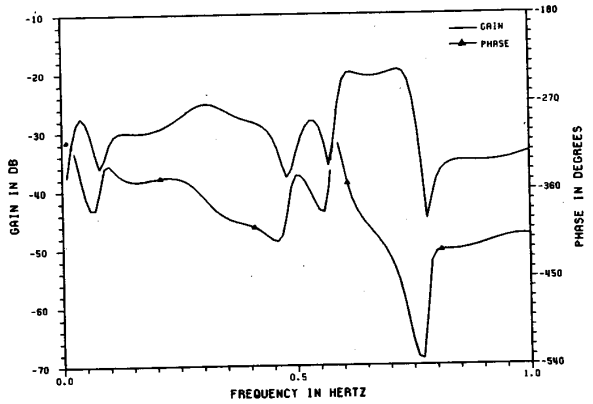

Fig. 3A. Frequency response for PRSCKS4 model #1

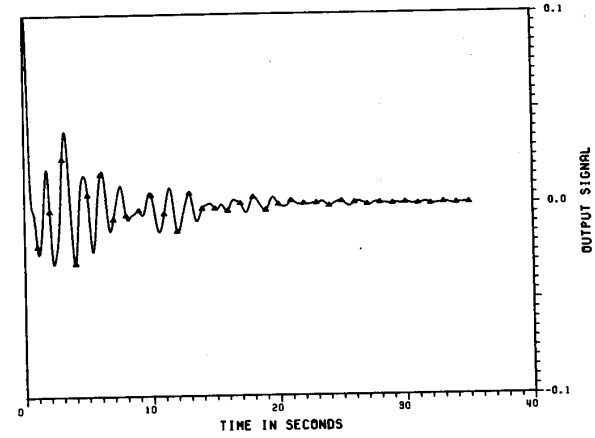

Fig. 3B. Impulse response of PRSCKS4 model #1

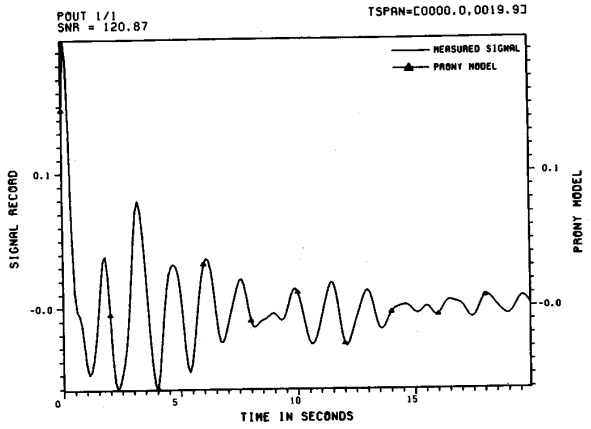

Fig. 4. Prony fit for PRSCKS4 model #1 TBAR = 20 seconds (200 samples)

spaced, as may be deduced from the beating effects in the impulse response of Figure 3B.

Figure 4 and Table I show typical SIGPAKZ outputs. The Figure 4 plot header indicates that the signal is named POUT 1/1, that it extends from 0.6 to 20.5 sec., and that the SNR for the PRS is 120.87 dB. This indicates an excellent fit, as can also be seen from the superposed curves. The corresponding PRS table reproduces the parent model data to 6 or 7 significant digits. The damping, for an eigenvalue $\lambda=\sigma+j\omega$, is displayed as $-\lambda/(2\pi)$.

*SIGNAL-TO-NOISE RATIO = 120.8700 FOR NMODES = 14

MODE	DAMPING	FRQ (HZ)	REL WT	PHASE	AMPLITUDE
1	0.0239805	0.0367401	0.2890819	30.119507	0.0144529
2	0.0318409	0.0912621	0.1865634	116.554008	0.0100207
3	0.0596168	0.3045262	0.4499747	-4.998126	0.0241690
4	0.0508920	0.4608535	0.3286152	-119.239242	0.0176505
5	0.0438688	0.5357940	0.5348253	0.052731	0.0287265
6	0.0227360	0.5975186	0.5201265	76.963143	0.0279370
7	0.0857313	0.7275286	1.0000000	-53.600270	0.0537119
8	0.0257093	0.7426974	0.6577225	174.971951	0.0353275
9	0.0633062	1.0428168	0.1417231	-84.687450	0.0076122
10	0.0560974	1.1506412	0.1704997	-21.813123	0.0091579
11	0.0176936	1.2396401	0.0785724	-86.217684	0.0042203
12	0.0265640	1.2919787	0.0757616	-28.926462	0.0040693
13	0.0384194	1.5015666	0.1254782	167.056914	0.0067397
14	0.1446441	1.6059325	0.4546648	-61.027965	0.0244209

TABLE I. PRS table for PRSCKS4 model #1
TBAR = 20 seconds (200 samples)

VI. ANALYSIS OF KEMANO GENERATOR RESPONSE

The Kemano generator, in northwestern British Columbia, attaches to the main power system through a long radial connection (see Figure 5). Kemano has a frequency-domain "signature" that is conspicuous throughout the western power system.

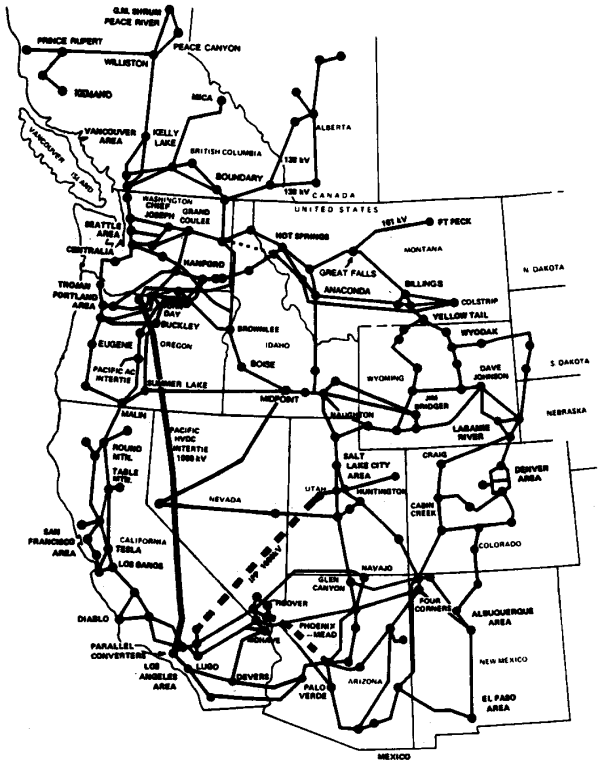

Fig. 5. General structure of the Western U.S. power system

Figure 6A shows the frequency response of Kemano generator power to the modulation of reactive load at the Malin 500 kv bus. This data was produced by Fourier analyzing the ringdown signal of Figure 6B, and dividing the results by the Fourier transform of the applied pulse. The single dominant peak makes

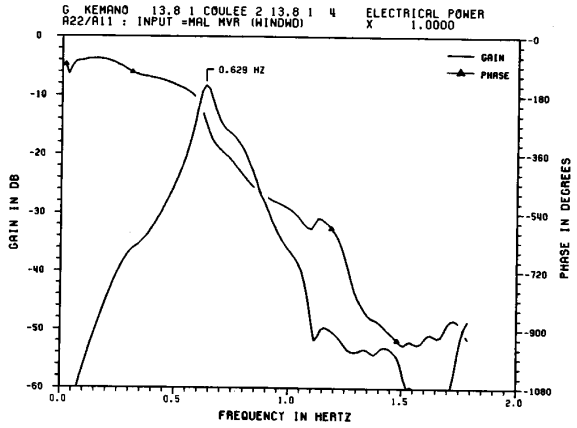

Fig. 6A. Frequency response of Kemano electrical power to shunt reactive control at Malin

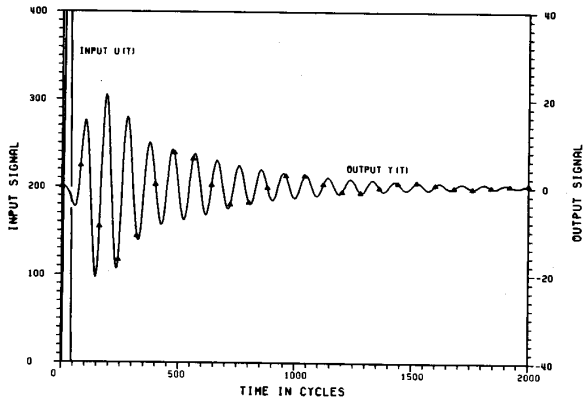

Fig. 6B. Kemano ringdown for brief Mvar load pulse at Malin

```
C  **PRONY S-TABLE FOR PRS NUMBER  1: TSPAN = C   44.00,  940.00]
C   *SIGNAL-TO-NOISE RATIO =    69.4550  FOR NMODES = 56
C    DISPLAY TRIM LEVEL=  0.10000E+00
C
C MODE     DAMPING     FRQ (HZ)       REL WT       PHASE        AMPLITUDE
C    4   0.1505401   0.4082269    0.1406290   54.908092     3.2476931
C    5   0.0214040   0.6289195    1.0000000 -178.260646    23.0940471
C    6   0.1032774   0.6833275    0.2172331 -118.146087     5.0167906
C    7   0.0761593   0.7818811    0.8187142    7.611984    18.9074243
C
C  **PRONY S-TABLE FOR PRS NUMBER  2: TSPAN = C   84.00,  980.00]
C   *SIGNAL-TO-NOISE RATIO =    75.6260  FOR NMODES = 56
C    DISPLAY TRIM LEVEL=  0.10000E+00
C
C MODE     DAMPING     FRQ (HZ)       REL WT       PHASE        AMPLITUDE
C    5   0.1894222   0.5557568    0.1753940   95.627236     3.6571974
C    6   0.0212416   0.6286833    1.0000000  -26.579108    20.8513308
C    7   0.0711585   0.7819447    0.5794028 -161.512752    12.0813190
C
C  **PRONY S-TABLE FOR PRS NUMBER  3: TSPAN = C  124.00, 1020.00]
C   *SIGNAL-TO-NOISE RATIO =    67.9670  FOR NMODES = 57
C    DISPLAY TRIM LEVEL=  0.10000E+00
C
C MODE     DAMPING     FRQ (HZ)       REL WT       PHASE        AMPLITUDE
C    6   0.0213526   0.6287557    1.0000000  124.125559    19.2038697
C    7   0.0724648   0.7764332    0.4830101   35.046527     9.2756624
C    9   0.2060205   0.8604318    0.1121199 -127.841332     2.1531365
C
C  **PRONY S-TABLE FOR PRS NUMBER  4: TSPAN = C  164.00, 1060.00]
C   *SIGNAL-TO-NOISE RATIO =    65.2870  FOR NMODES = 56
C    DISPLAY TRIM LEVEL=  0.10000E+00
C
C MODE     DAMPING     FRQ (HZ)       REL WT       PHASE        AMPLITUDE
C    5   0.0212042   0.6280298    1.0000000  -82.598303    17.3684915
C    6   0.0595462   0.7061285    0.1168124   68.606410     2.0288556
C    7   0.0877736   0.7698994    0.5908038 -143.795953    10.2613704
C   10   0.2326938   1.1937894    0.1068583  -48.942534     1.8559677
C
C  **PRONY S-TABLE FOR PRS NUMBER  5: TSPAN = C  204.00, 1100.00]
C   *SIGNAL-TO-NOISE RATIO =    72.8740  FOR NMODES = 56
C    DISPLAY TRIM LEVEL=  0.10000E+00
C
C MODE     DAMPING     FRQ (HZ)       REL WT       PHASE        AMPLITUDE
C    6   0.0215034   0.6284879    1.0000000   66.594427    16.1728315
C    7   0.0644864   0.7700647    0.2488102   55.219579     4.0239653
C    9   0.1962575   0.9072919    0.1158486  -38.773916     1.8735996
```

TABLE II. PRS tables for sliding-window fits to Kemano ringdown

Kemano a good initial case for testing SIGPAKZ against transient stability output data.

Full PRS tables for TSP or field test signals tend to be large, showing many modes that are weak or accessory to the fitting process. Signal offsets generally produce modes near 0 Hz or near the Nyquist frequency $1/(2\Delta t)$. Table II shows a sequence of PRS tables in which such modes have been supressed. Line 7 of the header indicates that all modes with a relative weight below (TRIMTAB =) 0.20 have been trimmed from the display. The normalization is performed with respect to the mode within a user-specified frequency range.

Linearized characteristics of stability output signals should be expected to vary with time (e.g., according to system stress). It is useful to examine such a signal by sliding a data window along it and processing the window contents (a sub-record) at preset positions. This provides an indication of dynamic variability, assists the identification of dominant modes, and checks the solution process for consistency. Table II and Figure 7 show results for a sliding-window analysis in which a 15 second (225 sample) window was advanced 10 samples (0.667 seconds) between successive solutions. These indicate that, consistent with the peak in Figure 6A, Kemano is strongly involved in a mode that is essentially fixed near 0.628 Hz, with a damping near 0.0212–0.0215. Kemano also participates in a strong mode near 0.77 Hz, which is either more variable or less accurately estimated.

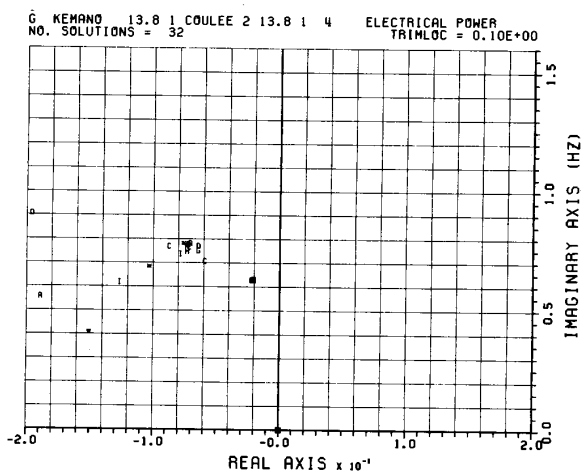

Fig. 7. PRS locus for sliding-window fits to Kemano ringdown

VII. MODE SHAPE VIA PRONY ANALYSIS

Figures 8–10 and Table III extend the analysis of Section VI to other "index" generators in the western system. The 0.628 Hz "Kemano Mode" is visible at each machine, both as a sharp peak in the frequency response and as a consistent mode in the PRS locus. The PRS tables show Grand Coulee and Shasta about 180 degrees behind Kemano for this mode, and Palo Verde about 370 degrees behind.

Except for Kemano, all signals show a significant mode near 0.76 Hz. The indicated damping for this mode is about 0.012–0.018—except at Grand Coulee, for which the damping is ten times higher. This result is persistent enough to raise the possibility

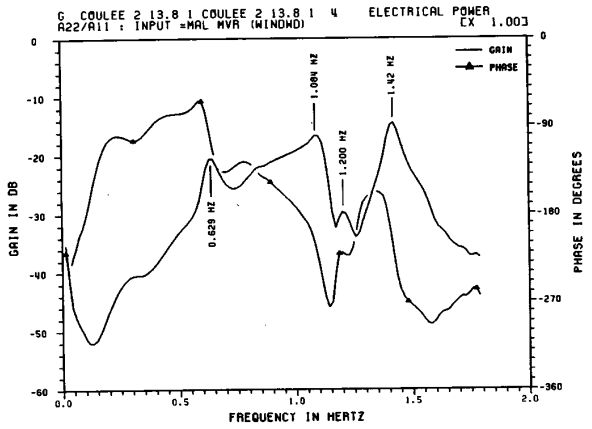

Fig. 8A. Frequency response of Grand Coulee electrical power to shunt reactive control at Malin

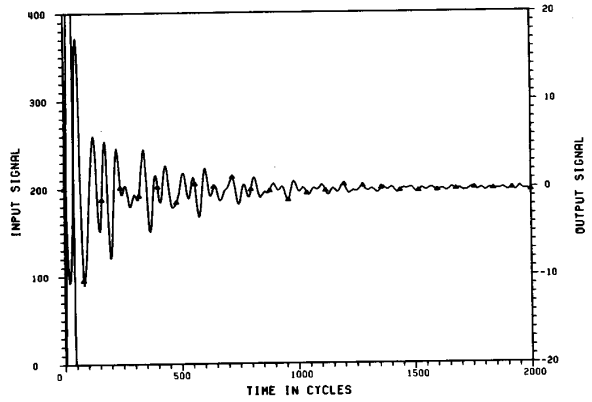

Fig. 8B. Grand Coulee ringdown for brief Mvar load pulse at Malin

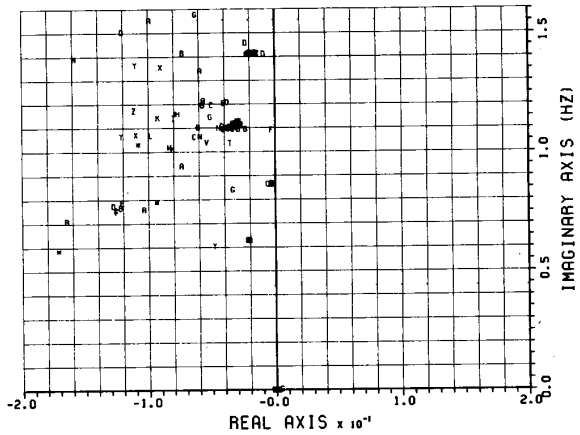

Fig. 8C. PRS locus for sliding-window fits to Grand Coulee ringdown

of 2 modes at essentially the same natural frequency. The PRS tables indicate that Shasta is swinging against Palo Verde.

Continuation of this analysis would provide a progressively better view of the phase distribution for the eigenvectors associated with key modes (for which machine electrical power is implicitly being taken as a state variable). Insight into the interaction mechanisms for each mode can be extended by examining complex power flow on major lines [16].

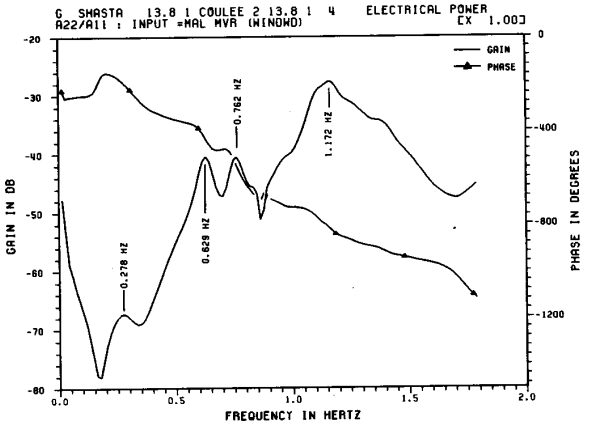

Fig. 9A. Frequency response of Shasta electrical power to shunt reactive control at Malin

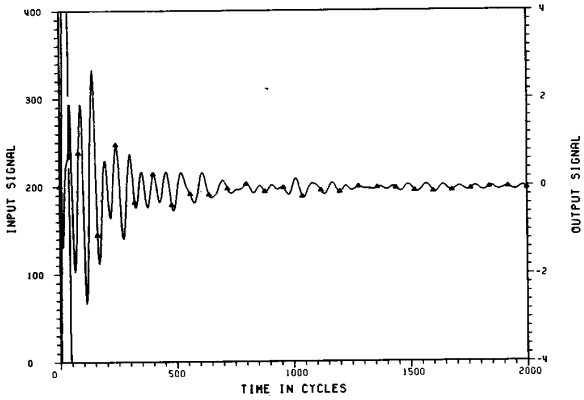

Fig. 9B. Shasta ringdown for brief Mvar load pulse at Malin

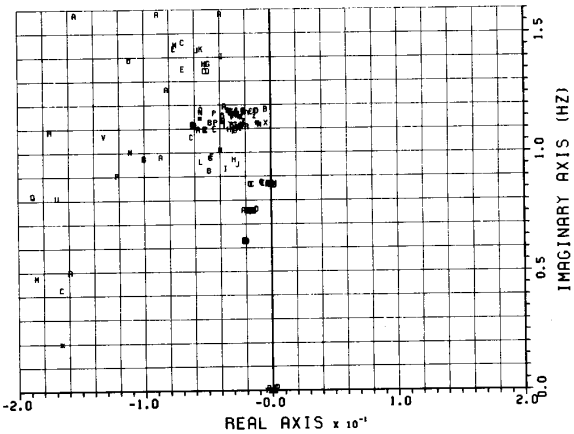

Fig. 9C. PRS locus for sliding-window fits to Shasta ringdown

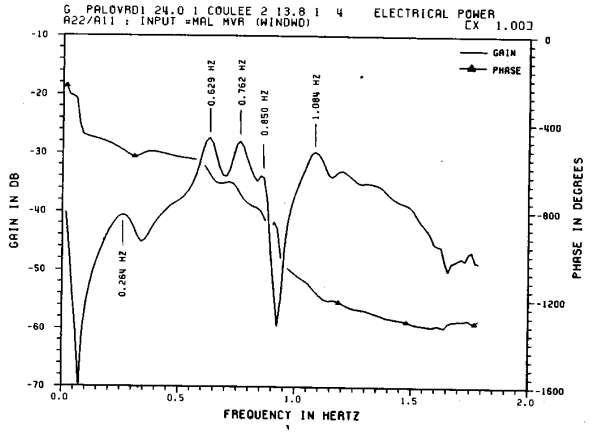

Fig. 10A. Frequency response of Palo Verde electrical power to shunt reactive control at Malin

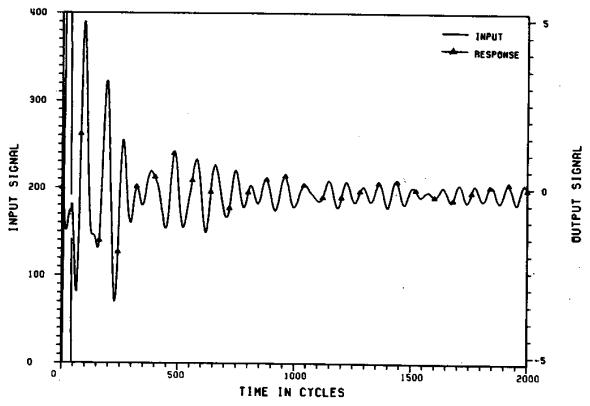

Fig. 10B. Palo Verde ringdown for brief Mvar pulse at Malin

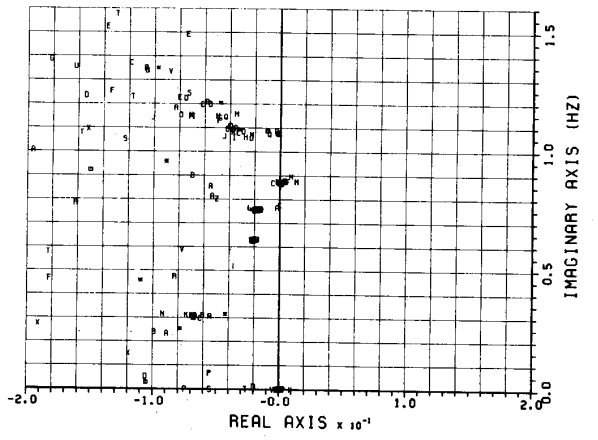

Fig. 10C. PRS locus for sliding-window fits to Palo Verde ringdown

```
C   COULEE 2 GENERATION
C
C  **PRONY S-TABLE FOR PRS NUMBER  1: TSPAN = [   44.00,   940.00]
C   *SIGNAL-TO-NOISE RATIO =    76.9200  FOR NMODES = 57
C    DISPLAY TRIM LEVEL=  0.10000E+00
C
C MODE     DAMPING      FRQ (HZ)      REL WT       PHASE        AMPLITUDE
C    5   0.1714490   0.5849845   0.6643203  -24.840629   8.5027202
C    6   0.0213050   0.6205543   0.2825898    2.211894   3.6169033
C    7   0.0935907   0.7885799   0.4576850   55.072924   5.8579688
C    9   0.1081152   1.0315457   0.3415994  -87.653386   4.3721745
C   10   0.0271046   1.1117995   0.3803402 -143.306714   4.8680235
C   12   0.0191384   1.4166899   0.2276238  -46.593526   2.9133867
C
C  **PRONY S-TABLE FOR PRS NUMBER  2: TSPAN = [   84.00,   980.00]
C   *SIGNAL-TO-NOISE RATIO =    62.2740  FOR NMODES = 57
C    DISPLAY TRIM LEVEL=  0.10000E+00
C
C MODE     DAMPING      FRQ (HZ)      REL WT       PHASE        AMPLITUDE
C    5   0.2252735   0.5064690   0.8847686 -169.312284   5.1761401
C    6   0.0208683   0.6284520   0.5496024  153.154691   3.2153256
C    7   0.1039441   0.7586371   0.8187653  -72.668157   4.7900024
C   10   0.0340882   1.1175964   1.0000000  106.202485   5.8502755
C   11   0.0570722   1.2150878   0.3604350  163.975121   2.1086440
C   12   0.0203240   1.4150188   0.4797156  -60.146025   2.8064682
C   13   0.0993880   1.5523321   0.1311808 -169.160932   0.7674439
C
C   SHASTA GENERATION
C
C  **PRONY S-TABLE FOR PRS NUMBER  1: TSPAN = [   44.00,   940.00]
C   *SIGNAL-TO-NOISE RATIO =    78.6570  FOR NMODES = 57
C    DISPLAY TRIM LEVEL=  0.10000E+00
C
C MODE     DAMPING      FRQ (HZ)      REL WT       PHASE        AMPLITUDE
C    3   0.1661619   0.1983947   0.1240524   -9.279089   0.3849469
C    6   0.0208332   0.6295718   0.1511941   -0.712765   0.4691701
C    7   0.0165324   0.7600899   0.1393316  -87.189048   0.4323598
C   11   0.0559060   1.1430360   1.0000000   57.416009   3.1030984
C
C  **PRONY S-TABLE FOR PRS NUMBER  2: TSPAN = [   84.00,   980.00]
C   *SIGNAL-TO-NOISE RATIO =    67.8140  FOR NMODES = 56
C    DISPLAY TRIM LEVEL=  0.10000E+00
C
C MODE     DAMPING      FRQ (HZ)      REL WT       PHASE        AMPLITUDE
C    4   0.1596379   0.4985244   0.1101860 -126.258983   0.2964681
C    5   0.0201413   0.6286822   0.1516459  152.893491   0.4080208
C    6   0.0139213   0.7565785   0.1245420  103.788616   0.3350946
C    8   0.0873423   0.9806037   0.3249831  -65.325787   0.8744046
C    9   0.0604547   1.1160129   1.0000000   -3.692468   2.6906155
C   13   0.1548299   1.5760160   0.1369206  153.373458   0.3684007
C
C   PALO VERDE GENERATION
C
C  **PRONY S-TABLE FOR PRS NUMBER  1: TSPAN = [   44.00,   940.00]
C   *SIGNAL-TO-NOISE RATIO =    71.0880  FOR NMODES = 56
C    DISPLAY TRIM LEVEL=  0.10000E+00
C
C MODE     DAMPING      FRQ (HZ)      REL WT       PHASE        AMPLITUDE
C    2   0.0784432   0.2537408   0.3884187 -125.115988   1.3952108
C    3   0.0427804   0.3159691   0.1138085   91.010410   0.3911532
C    4   0.1099590   0.4582658   0.3954828 -127.855330   1.3696758
C    5   0.0215942   0.6294444   0.6143338  167.280802   2.1276230
C    6   0.0222847   0.7580719   0.5303981  108.103273   1.8369283
C    8   0.6530660   0.9475308   1.0000000    1.590849   3.4633010
C    9   0.0902369   0.9586493   0.7930519 -146.442701   2.7465775
C   10   0.0326451   1.0931824   0.3866928   16.532271   1.2699675
C   11   0.0477920   1.2043322   0.1853706   -5.345485   0.6454575
C   12   0.0974320   1.3501417   0.2851505  -44.868328   0.9875622
C
C  **PRONY S-TABLE FOR PRS NUMBER  2: TSPAN = [   84.00,   980.00]
C   *SIGNAL-TO-NOISE RATIO =    62.4910  FOR NMODES = 56
C    DISPLAY TRIM LEVEL=  0.10000E+00
C
C MODE     DAMPING      FRQ (HZ)      REL WT       PHASE        AMPLITUDE
C    2   0.0892829   0.2331630   0.1595470  -20.028538   0.7401031
C    3   0.0551856   0.3072306   0.1606265 -173.803898   0.7451106
C    5   0.0187972   0.6302957   0.3667230  -46.289754   1.7011466
C    6   0.0023850   0.7646566   0.1266312 -110.013522   0.5874139
C    7   0.0540874   0.8138000   0.6002149 -110.655109   2.7842636
C    9   0.1960338   1.0045698   1.0000000   39.799072   4.6387779
C   10   0.0360547   1.0991668   0.2843185  -99.646175   1.3188904
C   11   0.0584623   1.2081364   0.1717699  -96.377748   0.7968022
C   12   0.1070655   1.3505243   0.1828986  -87.170322   0.8484261
```

TABLE III. PRS tables for sliding-window fits to generator ringdowns

VIII. EVALUATION OF REMEDIAL ACTION SCHEMES VIA PRONY ANALYSIS

This section treats two separate large-signal stability cases involving loss of the 3100 MW Celilo-Sylmar HVDC Intertie. In the reference case only standard remedial actions are taken, and growing oscillations occur at the Malin 500 kv bus. These same actions are taken in the experimental case. In addition, a 1000 MW discharge is taken from a fictional superconducting magnetic energy storage (SMES) unit near the Sylmar terminal of the Pacific HVDC Intertie. In this scenario the unit can serve as a spinning reserve equivalent for 2 minutes.

Comparison of Figures 11A and 11B shows that the SMES power injection into the grid has reduced the level of the oscillations, and that it may have improved their damping. A rough indication of their modal content is provided by the (unscaled) autospectra of Figures 12A and 12B, which show that the injection has also affected the natural frequency of the

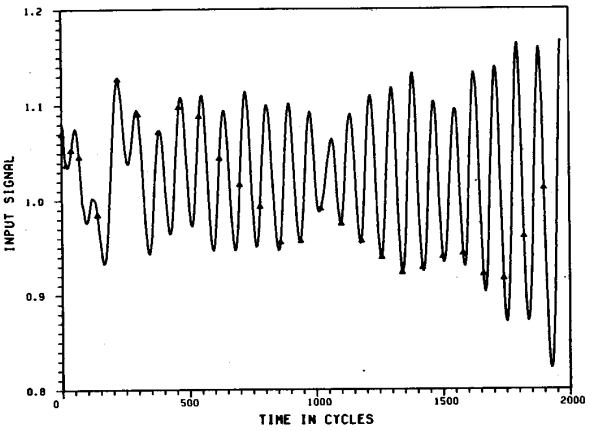

Fig. 11A. Malin voltage swings following 3100 mw hvdc bipole loss (no SMES pulse)

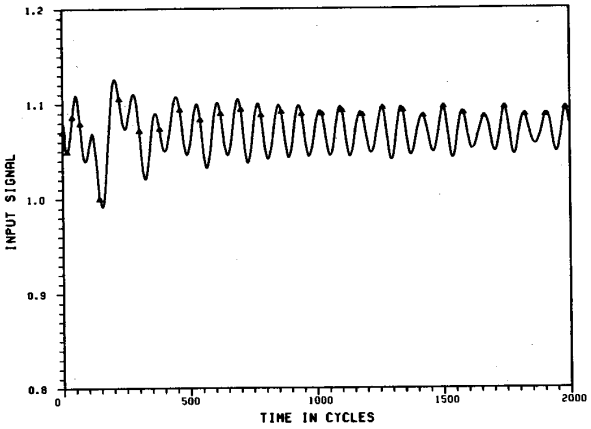

Fig. 11B. Malin voltage swings following 3100 mw hvdc bipole loss (1000 MW SMES pulse)

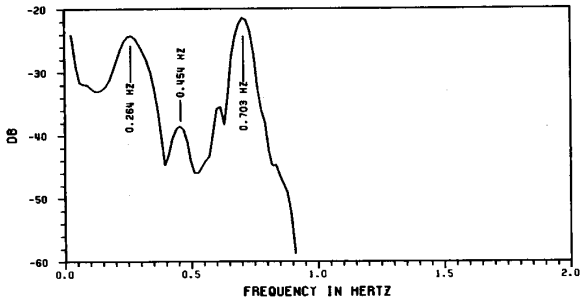

Fig. 12A. Autospectrum of Malin voltage swings (no SMES pulse)

critical modes near 0.27 Hz and 0.70 Hz. The associated PRS tables and PRS loci (Figures 13A,B) display these effects more clearly, in a quantitative format well suited to the refinement of pulse level and timing.

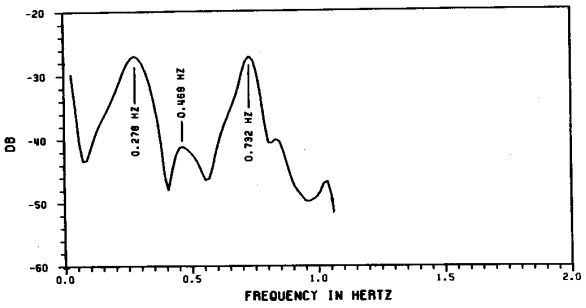

Fig. 12B. Autospectrum of Malin voltage swings (1000 MW SMES pulse)

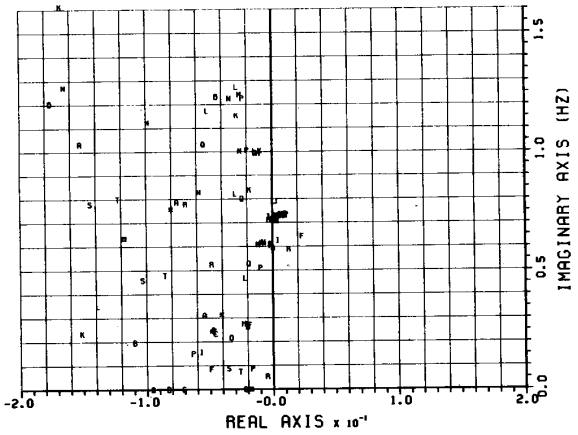

Fig. 13A. PRS locus for sliding-window fits to Malin voltage (no SMES pulse) TBAR = 15 seconds (225 samples)

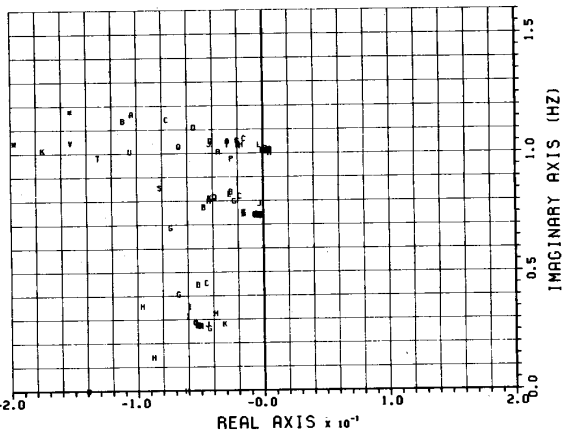

Fig. 13B. PRS locus for sliding-window fits to Malin voltage (1000 MW SMES pulse) TBAR = 15 seconds (225 samples)

IX. CONCLUSIONS

Prony analysis--and SIGPAKZ in particular--have already proven useful in the direct modal analysis of power system response signals at BPA. The next phase of development will emphasize application guidelines

and computational efficiency. The latter is strongly affected by model order, which incurs n-cubed complexity costs during singular-value decompositions.

While Prony analysis may well assume a place alongside eigenanalysis and Fourier methods, it will certainly not replace them. Each such tool has its own merits and applications, and provides a different view into dynamic system behavior.

REFERENCES

[1] G.R.B. Prony, "Essai experimental et analytic ...," J. 1'Ecole Polytech. (Paris), vol. 1, pp. 24-76, 1795.

[2] F.B. Hildebrand, "Introduction to Numerical Analysis." New YorK: McGraw-Hill, 1956. (See esp. Chapter 9.)

[3] S.M. Kay and S.L. Marple, "Spectrum analysis—a modern perspective," Proc. IEEE, pp. 1380-1419, Nov. 1981.

[4] A.J. Poggio, M.L. Van Blaricum, E.K. Miller, and R. Mittra, "Evaluation of a processing technique for transient data," IEEE Trans. Antennas and Propagation, pp. 165-173, January 1987.

[5] M.L. Van Blaricum and R. Mittra, "Problems and solutions associated with Prony's method for processing transient data," IEEE Trans. Antennas and Propagation, pp. 174-182, January 1978.

[6] D.W. Tufts and R. Kumaresan, "Singular value decomposition and improved frequency estimation using linear prediction," IEEE Trans. Acoustics, Speech, and Signal Processing, pp. 671-675, Aug. 1982.

[7] D.W. Tufts and R. Kumaresan, "Frequency estimation of multiple sinusoids: making linear prediction perform like maximum likelihood," Proc. IEEE, pp. 975-989, Sept. 1982.

[8] R. Kumaresan and D.W. Tufts, "Estimating the parameters of exponentially damped sinusoids and pole-zero modeling in noise," IEEE Trans. Acoustics, Speech, and Signal Processing, pp. 833-840, Dec. 1982.

[9] R. Kumaresan, "On the zeros of the linear prediction-error filter for deterministic signals," IEEE Trans. Acoustics, Speech, and Signal Processing, pp. 217-220, Feb. 1983.

[10] R. Kumaresan, D.W. Tufts, and L.L. Scharf, "A Prony method for noisy data: choosing the signal components and selecting the order in exponential signal models," Proc. IEEE, pp. 230-233, February 1984.

[11] R. Kumaresan, L.L. Scharf, and A.K. Shaw, "An algorithm for pole-zero modeling and spectral analysis," IEEE Trans. Acoustics, Speech, and Signal Processing, pp. 637-640, June 1986.

[12] H.P. Frisch and F.H. Bauer, "Modern Numerical Methods for Classical Sampled Systems Analysis-SAMSAN II User's Guide." NASA/Goddard Space Flight Center, Greenbelt, Maryland, 1984. [COSMIC Program #GSC-12827]

[13] J.F. Hauer, "An Overview of BPA Software for Signal Processing and Other Systems Analysis Tasks Involved in Identification and Control of Power System Dynamics," letter to the WSCC 0.7 Hz Oscillation Ad Hoc Work Group, Nov. 16, 1987.

[14] J.F. Hauer, "Description of Reduced-Scale FFT Software Package SIG-PAKR," BPA working notes, May 23, 1988. Distributed to the WSCC 0.7 Hz Ad Hoc Work Group, June 6, 1988.

[15] T. Kailath,"Linear Systems. Prentice-Hall: Englewood Cliffs, 1980.

[16] J.F. Hauer, "Initial Results in the Use of Prony Methods to Determine the Damping and Modal Content of Power System Dynamic Response Signals," BPA Technical Report, October 5, 1988.

[17] B. Friedlander, "Lattice methods for spectral estimation," Proc. IEEE, pp. 990-1017, Sept. 1982.

[18] S. Li and B.W. Dickinson, "Application of the lattice filter to robust estimation of AR and ARMA models," IEEE Trans. Acoustics, Speech, and Signal Processing, pp. 502-512, April 1988.

[19] P. Strobach, "Recursive covariance ladder algorithms for ARMA system identification," IEEE Trans. Acoustics, Speech, and Signal Processing, pp. 560-580, April 1988.

[20] J.F. Hauer, "Fast Damping Estimators for Use with the Transient Stability Program," BPA Memorandum, Feb. 20, 1987. Communicated to the WSCC 0.7 Hz Ad Hoc Work Group on October 22, 1987.

[21] J.F. Hauer, "Reactive Power Control as a Means for Enhanced Interarea Damping in the Western U.S. Power System—A Frequency-Domain Perspective Considering Robustness Needs," invited paper in Application of Static Var Systems for System Dynamic Performance, IEEE Publication 87TH0187-5-PWR, pp. 79-92. Proceedings of a symposium presented at the IEEE PES 1987 Winter Meeting, New Orleans, LA, and at the IEEE PES 1987 Summer Meeting, San Francisco, CA.

[22] J.F. Hauer, "Robust Damping Controls for Large Power Systems," IEEE Control Systems Magazine, pp. 12-19, January 1989.

John F. Hauer (S'59-SM'87) was born in Washington State in 1936. He received the B.S. degree (summa) at Gonzaga University in 1961, and the Ph.D. degree at the University of Washington as a National Science Foundation Graduate Trainee in 1968. Both degrees were in electrical engineering.

In 1961 and 1962 he was with the General Electric Company, working in the area of nuclear reactor controls while enrolled in the Advanced Engineering Training Program. In 1963 and 1964 he developed spacecraft navigation and guidance methods at the Boeing Company, for use in Lunar Orbiter design and mission control. His subsequent doctoral research addressed methods for designing safety factors into thrusting trajectories for interplanetary flight. From 1968 to 1975 he was a member of the Computing Science faculty at the University of Alberta, where he became an associate professor in 1972. His teaching responsibilities and research activities

there centered upon constrained optimization of dynamic systems. Since 1975 he has been with the Bonneville Power Administration, where his work deals with the identification, analysis and control of power system dynamics.

Dr. Hauer is a member of the IEEE Power Engineering and Control Systems Societies.

Louis L. Scharf received the PH.D degree in Electrical Engineering from the University of Washington, Seattle, in 1969.

From 1969 to 1971, he was a member of the Technical Staff at Honeywell's Marine Systems Center in Seattle. He was a Faculty member at Colorado State University, Fort Collins, from 1971 to 1981, where he last served as a Professor of Electrical Engineering at the University of Rhode Island, Kingston. He is currently a Professor of Electrical and Computer Engineering at the University of Colorado, Boulder, where he teaches and conducts research in signal processing. In 1974 he was a Visiting Associate Professor at Duke University, Durham, NC. In 1977 he was at the University of South Paris, Orsay, where he was a member of the Technical Staff in the CNRS Laboratoire des Signaux et Systemes, Gif-sur-Yvette. In 1981 he was a Visiting Professor Superieure des Telecommunications, Paris. He has served as a Consultant to Honeywell Inc., the Applied Physics Labs., Seattle, the Research Triangle Institute, Green Mountain Geophysics, and Ball Aerospace Corporation.

Dr. Scharf is a past member of the ASSP ADCOM and the Editorial Board of Signal Processing. He is a past Associate Editor for the IEEE Transactions on Acoustics, Speech, and Signal Processing. He was the Technical Program Chairman for the 1980 International Conference on ASSP. He is a member of Eta Kappa Nu.

Cedric J. Demeure was born in Bruxelles, Belgium, on September 11, 1960. He received the Engineering degree from the Ecole Nationale Superieure des Telecommunications, Paris, France, in 1983, the M.S. degree from the University of Rhode Island, Kingston, RI, in 1984 and the Ph.D degree from the University of Colorado (Boulder) in 1988, all in Electrical Engineering. In 1985, he worked for the radar branch of Thomson-CSF, Pairs, France, as research engineer in signal processing.

He is currently working in the Department of Electrical and Computer Engineering at the University of Colorado (Boulder), as a research associate and a lecturer. His main research interests are Digital Signal Processing, Statistical Modeling, and fast algorithms.